
CHAPTER - 6

ESTIMATION OF WHEAT CROP VARIABLES USING BISTATIC SCATTEROMETER DATA AND ARTIFICIAL NEURAL NETWORKS

ESTIMATION OF WHEAT CROP VARIABLES USING BISTATIC SCATTEROMETER DATA AND ARTIFICIAL NEURAL NETWORKS

6.1 INTRODUCTION

The radar remote sensing is an interesting tool for the monitoring of agricultural areas and the estimation of its biophysical parameters. The microwave remote sensing has data acquisition capability at all the time and in all weather conditions on a regular basis (Toure et al. 1994b).

Mattia et al.(2003) showed the relationship between backscattering coefficients with wheat crop biomass and the underlying soil moisture content at C-band. They conducted a ground-based scatterometer experiment on a wheat field during winter wheat growing season at HH- and VV- polarization in the range of incidence angles from 23° to 60°. This study describes the radar sensitivity to biophysical parameters of wheat crop at different polarizations, incidence angles and different wheat phenological stages. Kim et al.(2014) have analyzed a time series of backscattering coefficient data, Radar vegetation index (RVI), and crop growth data collected using a ground-based multi frequency (L-, C-, and X-bands) polarimetric radar system. They found the RVI increased for all bands in accordance with the growth of wheat crop variables and decreased with a reduction of vegetation water content (VWC) and fresh weight. Brown et al.(2003) carried out an indoor polarimetric measurement using the ground-based synthetic aperture radar (GB-SAR). The measurements provide three-dimensional images of the scattering processes in wheat canopies, at X- and C-band. The scattering shows a pronounced layered structure of wheat crop with strong returns from the soil and the flag leaves, and in some cases a second leaf layer.

The recent interest increases toward the bistatic and multistatic radar measurement for the monitoring of the agricultural crops in the world community of researchers/scientists working in the field of microwave remote sensing. It is needed to gather the information concerning the bistatic polarimetric scatterometer system for the monitoring and estimation of biophysical parameters of agricultural crops. Unfortunately, a little information is available describing the bistatic scattering

behavior of agricultural crops. Now, it is needed to explore the potential of bistatic radar to investigate the vegetation properties of agricultural area. Gupta et al.(2015) have proposed the capability of a feed forward back propagation artificial neural network (FFBPANN) for the estimation of rice crop variables using two different bistatic ground based scatterometer data set (single polarized and dual polarized data set). The estimated values (biomass, leaf area index, plant height and SPAD value) by FFBPANN have been found very close to the observed values of rice crop variables using dual polarized data set in comparison to the single polarized data set. Rossi and Erten (2015) have evaluated the potential of spaceborne bistatic interferometric synthetic aperture radar images for the monitoring of biophysical variables of paddy rice. They studied the impact of interferometric phase, amplitude, interferometric coherence thresholding and polarization of the signal to estimate the temporal changes of the height of paddy rice crop. They found a direct relationship between interferometric phase and rice growth. The very high coherence of TanDEM-X data yields elevation estimates with root-mean-square error in a decimetric level, supporting temporal change analysis on a field-by-field basis.

The present study presents bistatic scattering signature of various growth stages of wheat crop at X-band for HH- and VV-polarization. The artificial neural network was used to estimate the wheat crop variables using bistatic scatterometer data. The objectives of the present study were (i) to determine the suitable bistatic scatterometer configuration for the accurate estimation of wheat crop variables using artificial neural network (ii) to estimate the wheat crop variables using bistatic scatterometer data and artificial neural network.

6.2 METHODS AND OBSERVATIONS

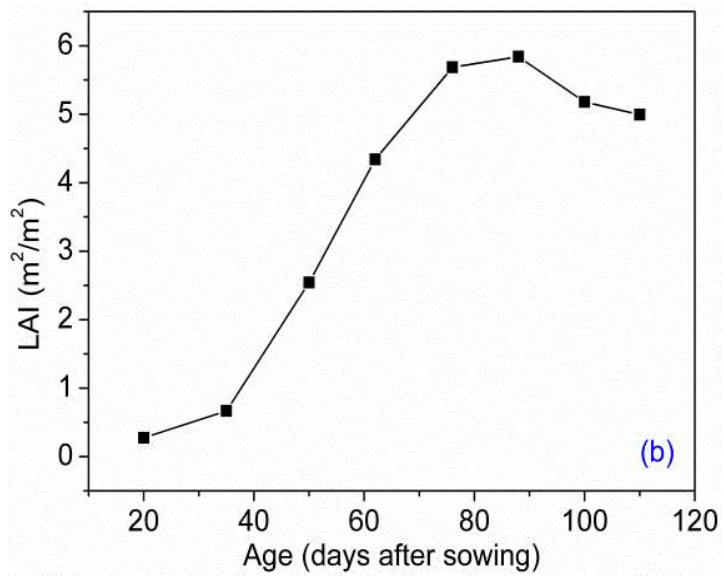
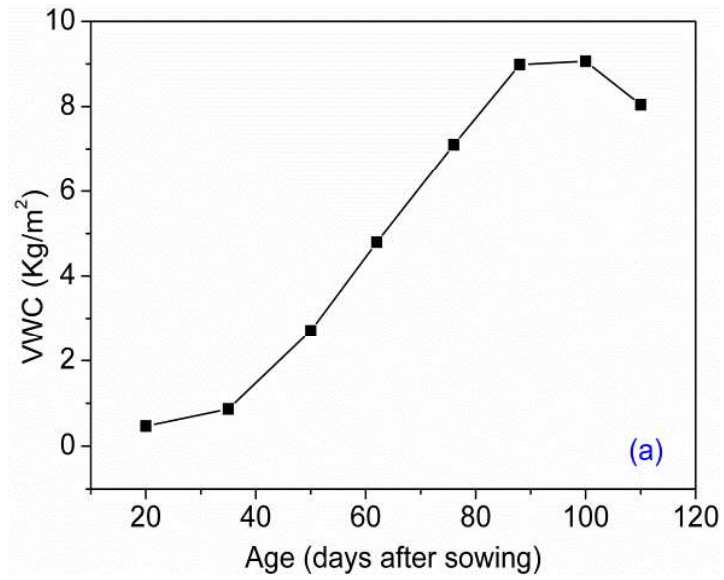
Wheat crop is taken as a narrow leaf crop. It attained maximum average height of 76 ± 2 cm in our crop bed during the entire observations. The maturity age of crop was found to be 110 ± 5 days after the date of sowing. The wheat crop variables namely vegetation water content (VWC), leaf area index (LAI), plant height (PH), SPAD value, grain biomass, grain water content (GWC) were measured at 8 different

growth stages. Table 6.1 shows the measured soil moisture content and wheat crop variables during entire growth period of wheat crop.

Table 6.1 Wheat crop variables at its various growth stages

Date/days after sowing →		Jan.20 /20	Feb.04 /35	Feb.19 /50	Mar.03 /62	Mar.17 /76	Mar.29 /88	Apr.10 /100	Apr.20 /110
LAI		0.273	0.668	2.544	4.340	5.687	5.840	5.180	4.995
Biomass (kg/m ²)	Wet	0.662	1.166	3.497	5.878	9.030	11.304	12.359	12.585
	Dry	0.191	0.298	0.785	1.083	1.929	2.318	3.295	4.544
VWC (kg/m ³)		0.471	0.868	2.712	4.795	7.101	8.986	9.064	8.041
Grain Biomass	Wet	--	--	--	--	--	--	2.781	3.391
	Dry	--	--	--	--	--	--	1.064	1.606
Grain water content (GWC)		--	--	--	--	--	--	1.717	1.785
Plant height (cm)		12	22	39.4	45	55	74	78	76
SPAD Value		33.90	35.500	39.600	42.100	43.300	44.900	43.800	41.400
SM (%)		12.840	10.330	12.330	11.350	11.910	12.50	11.160	12.150

Figure 6.1 (a-d) shows the temporal variation of wheat crop variables like vegetation water content (VWC), leaf area index (LAI), plant height (PH) and SPAD value at its various growth stages. Figure 6.2 shows the photographs of wheat crop for its various growth stages. All the crop variables were found to increase with the age of crop. The VWC was found to increase until 100 days after sowing and then started slight decreasing. The PH increases continuously till 100 days after sowing of wheat crop and then after it attended approximately constant behavior till the maturity. The leaf area index of wheat is found to increase sharply after 35 days of sowing and continued till 88 days then after it decreases. The values of SPAD are found to increase upto 88 days of growth stages after sowing and decreased at latter stages. Average crop covered soil moisture (SM) in the crop bed is found to be 11.83% gravimetric. The bistatic scatterometer measurement is also carried out at these 8 different growth stages of wheat crop. The detailed procedure for the measurement of wheat crop variables and bistatic scatterometer is given in Chapter 2.



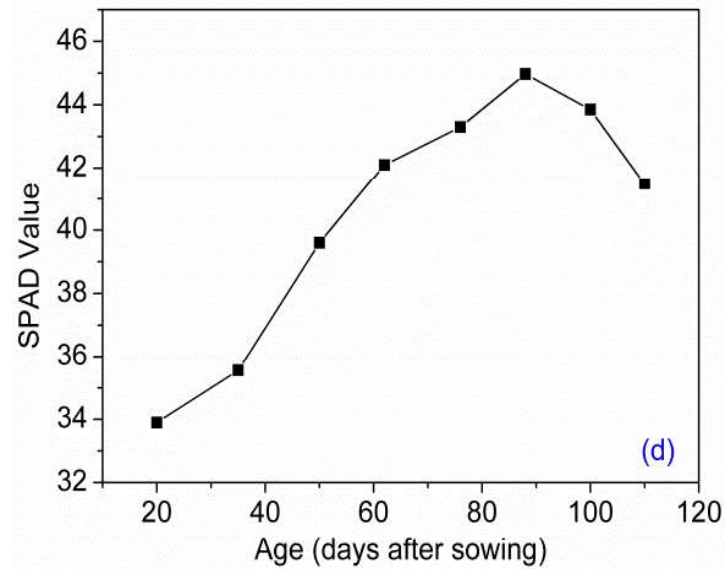
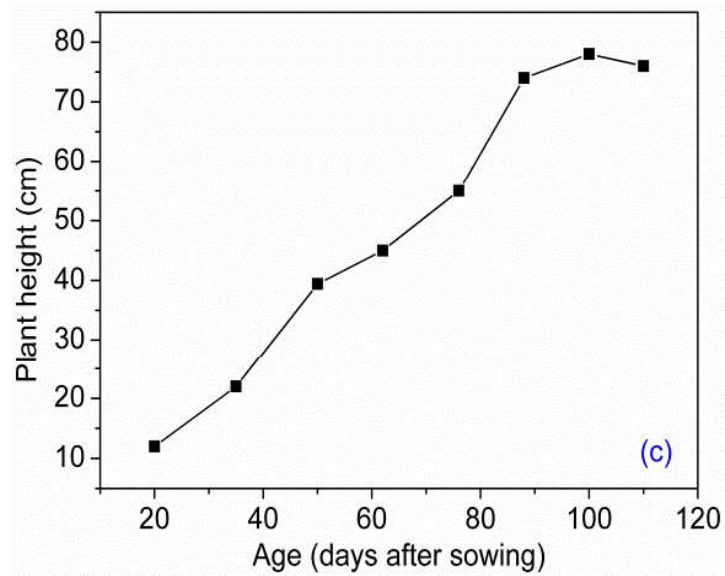


Figure 6.1 Temporal variations of wheat crop variables for (a) VWC (b) LAI (c) plant height and (d) SPAD value



Figure 6.2 Photographs of wheat crop at various growth stages

6.3 ARTIFICIAL NEURAL NETWORK

The descriptions of artificial neural networks used in the present study are summarized in Table 6.2. The gradient descent algorithm was used for the training of artificial neural networks. The training of the ANN model was done by feeding of input vector containing bistatic scattering coefficient and the output vector containing wheat crop variables.

The number of neurons at input and output layer of ANN model may be equal to the number of input-output parameters in the data sets. The number of neurons at hidden layer may vary for the optimization of ANN model to achieve accurate retrieval of crop variables. The number of hidden layers and number of neurons in each hidden layer were chosen by error-trail method. In the error- trail method, the ANN model was simulated for different values of number of neuron in the hidden layer and root mean squared error was continuously checked watched. The optimum number of neurons in the hidden layer was taken. Finally, the ANN model was developed with 1 neuron at input layer, 10 neurons at hidden layer and 1 neuron at output layer for the estimation of wheat crop variables.

The activation function at each layer of the ANN is also important. The hyperbolic tangent transfer function (*tansig*) was found better as an activation function at hidden layer neurons. The linear transfer function (*purelin*) was used as an activation function at the output layer neurons. The learning rate was taken 0.4 for the ANN model. Figure 6.3 shows the architecture of ANN model used in our investigation.

Table 6.2 Optimized ANN model parameters

Optimum parameters	HH- polarization	VV-polarization
Type of ANN model	BPANN	BPANN
Number of hidden layers	1	1
Number of neurons at hidden layer	10	10
Number of neurons at output layer	1	1
Transfer function at hidden layer	Hyperbolic tangent sigmoidal (<i>tansig</i>)	Hyperbolic tangent sigmoidal(<i>tansig</i>)
Transfer function at output layer	Linear (<i>purelin</i>)	Linear (<i>purelin</i>)
Training algorithms	Gradient descent	Gradient descent
Momentum	0.9	0.9
Learning rate	0.4	0.4

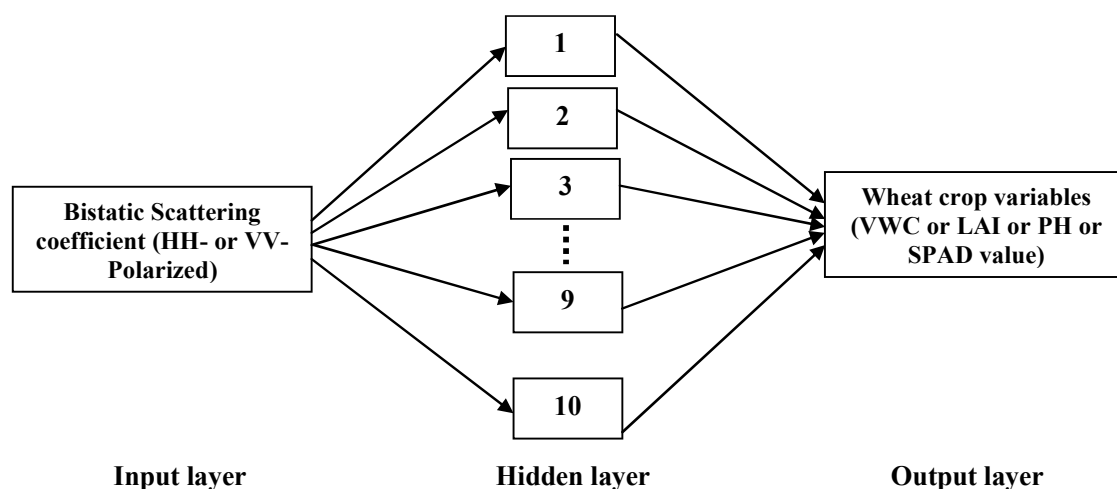


Figure 6.3 Architecture of ANN model used in the present study

6.4 RESULT AND DISCUSSIONS

6.4.1 TEMPORAL VARIATION OF BISTATIC SCATTERING COEFFICIENTS

Figures 6.4 and 6.5 show the angular variation of bistatic scattering coefficients at various growth stages of the wheat crop for like polarizations (HH-& VV-) at X-band, respectively. The magnitudes of bistatic scattering coefficients were found to decrease with the incidence angle at each growth stage of the wheat crop for both the like polarizations. The difference in dynamic range of bistatic scattering coefficient at various growth stages of wheat crop is found sufficient to discriminate all the growth stages of wheat crop. The soil moisture content in the crop bed was taken almost constant during entire observation.

When the values of wheat crop variable were small (VWC= 0.471 kg/m², LAI= 0.273 m²/m², PH = 12 cm and SPAD= 33.91) after 22 days of sowing, the dynamic ranges of bistatic scattering coefficient were found to be 6 dB and 6.27 dB at HH- and VV-polarizations, respectively. Whereas, when the wheat crop variables were high (VWC= 9.064 kg/m², LAI= 5.84 m²/m², PH = 78 cm and SPAD= 44.9) after 100 days of sowing, the dynamic ranges of bistatic scattering coefficient were decreased to 1.11 dB and 0.36 dB at HH- and VV-polarizations, respectively.

At the early age of wheat crop, the dynamic range of bistatic scattering coefficient was found to be greater than that of older age of the crop. Therefore, at the early age of crop, soil moisture effect on bistatic scattering coefficient was found to be more prominent than the crop effect. The decrease in the dynamic range of bistatic scattering coefficient with the age of crop indicates the dominance of the crop effect relative to the soil moisture effect at the latter growth stages of the crop. Thus, the angular trends were found flatter with the age of crop. Due to screening effect of the developing vegetation parameters on the contribution of soil.

Tables 6.3 and 6.4 show the linear regression results for the angular variation of bistatic scattering coefficient with the wheat crop variables at both the polarizations. The value of coefficient of determination (R^2) shows the percentage of sensitivity of bistatic scattering coefficient on the wheat crop variables. All wheat

crop variables and bistatic scattering coefficients showed good correlation at higher incidence angles. The maximum values of R^2 were found at 40° incidence angle for all the crop variables at HH- and VV- polarization. The higher sensitivity of bistatic scattering coefficients was found at HH-polarization in comparison to VV-polarization for all the wheat crop variables except LAI.

6.4.2 ESTIMATION OF WHEAT CROP VARIABLES

The estimation process of the wheat crop variables is presented in Figure 6.6. The measured data sets at 40° incidence angle (bistatic scattering coefficients and wheat crop variables) were interpolated into 91 data sets for each day between 20 to 110 days after sowing of wheat crop. The $2/3^{\text{rd}}$ part of the interpolated data sets were used for the training of the ANN model while the remaining $1/3^{\text{rd}}$ part of the interpolated data sets were used for the validation of the ANN model.

A multilayer back propagation artificial neural network (BPANN) was developed for the estimation of each wheat crop variables at HH- and VV-polarization. The eight BPANN models were used for the training using training data sets for the estimation of wheat crop variables at both the polarization. The procedure for the training of ANN models is given in the Section 6.3.

The validation data sets were used for the estimation of wheat crop variables by developed ANN models for each crop variable at both the like polarization. The performances of the trained ANN models were evaluated in terms of performance indices (coefficient of determination (R^2), RMSE and %bais). The performance indices were computed between estimated and observed values of wheat crop variables. Figure 6.7 (a-d) shows the 1:1 axes plot between estimated values and observed values of each wheat crop variables at HH-polarization. Figure 6.8 (a-d) shows the 1:1 axes plot between estimated and observed values of each wheat crop variables at VV-polarization. These figures also show the values of performance indices between estimated and observed values of wheat crop variables.

The VWC is found better estimated crop variable than the other crop variables at HH- and VV- polarization by ANN. The estimation of wheat crop variables is found better at HH- polarization than VV-polarization.

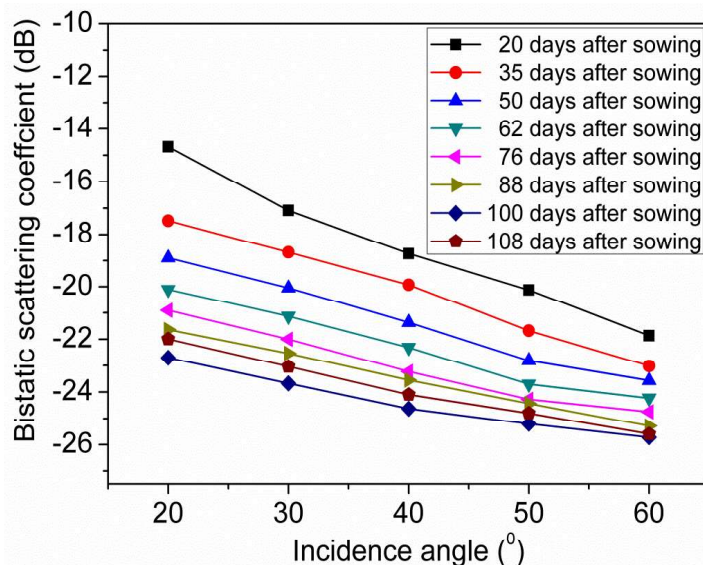


Figure 6.4 Angular variation of bistatic scattering coefficient for wheat crop at different growth stages for HH- polarization at X-band

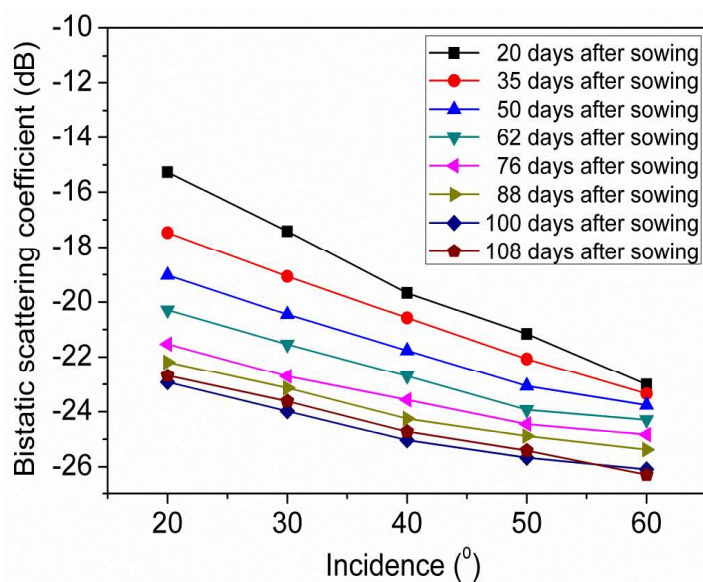


Figure 6.5 Angular variation of bistatic scattering coefficient for wheat crop at different growth stages for VV- polarization at X-band

Table 6.3 Results of regression analysis between bistatic scattering coefficients and wheat crop variables at different incidence angles for X-band at HH- polarization

Incidence angle →		20°	30°	40°	50°	60°
VWC	R ²	0.899	0.930	0.940	0.934	0.918
	Std. Err.	1.191	1.212	1.218	1.214	1.204
	Std. Err. Of Est.	1.055	0.876	0.810	0.852	0.950
LAI	R ²	0.773	0.834	0.839	0.786	0.785
	Std. Err.	0.696	0.723	0.724	0.702	0.701
	Std. Err. Of Est.	0.995	0.851	0.840	0.966	0.969
Plant height	R ²	0.966	0.977	0.982	0.981	0.947
	Std. Err.	8.739	8.787	8.812	8.809	8.654
	Std. Err. Of Est.	4.309	3.566	3.098	3.174	5.382
SPAD value	R ²	0.703	0.768	0.773	0.718	0.680
	Std. Err.	1.182	1.235	1.239	1.194	1.162
	Std. Err. Of Est.	2.030	1.794	1.776	1.979	2.108

Table 6.4 Results of regression analysis between bistatic scattering coefficients and wheat crop variables at different incidence angles for X-band at VV- polarization

Incidence angle →		20°	30°	40°	50°	60°
VWC	R ²	0.887	0.906	0.931	0.903	0.932
	Std. Err.	1.183	1.196	1.212	1.194	1.213
	Std. Err. Of Est.	1.113	1.016	0.872	1.033	0.866
LAI	R ²	0.697	0.798	0.876	0.839	0.845
	Std. Err.	0.661	0.707	0.740	0.725	0.727
	Std. Err. Of Est.	1.151	0.941	0.736	0.838	0.824
Plant height	R ²	0.961	0.972	0.973	0.960	0.956
	Std. Err.	8.547	8.647	8.658	8.541	8.507
	Std. Err. Of Est.	6.465	5.458	5.339	6.525	6.827
SPAD value	R ²	0.596	0.688	0.752	0.734	0.746
	Std. Err.	1.088	1.169	1.223	1.208	1.218
	Std. Err. Of Est.	2.370	2.080	1.854	1.921	1.876

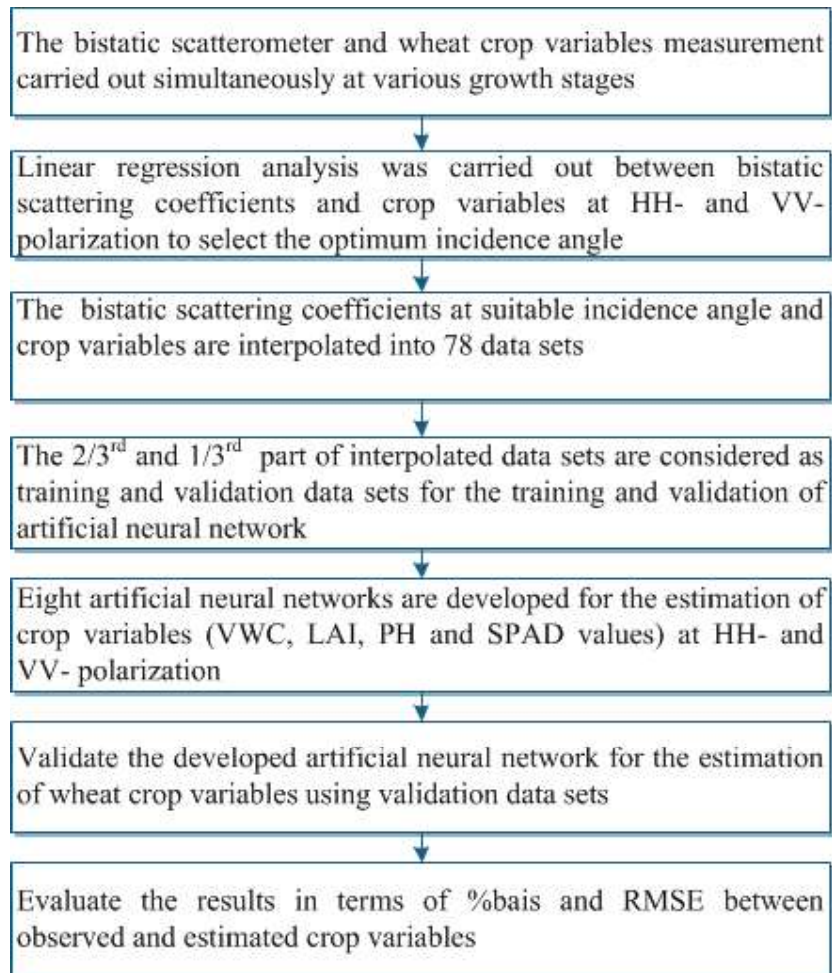
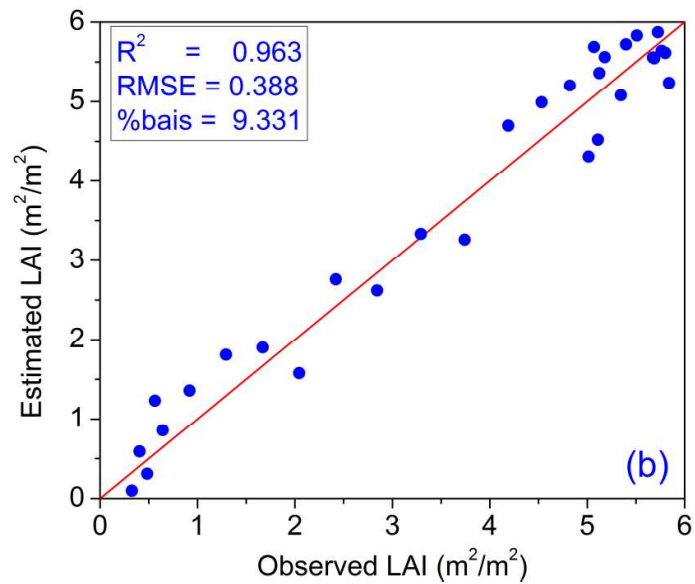
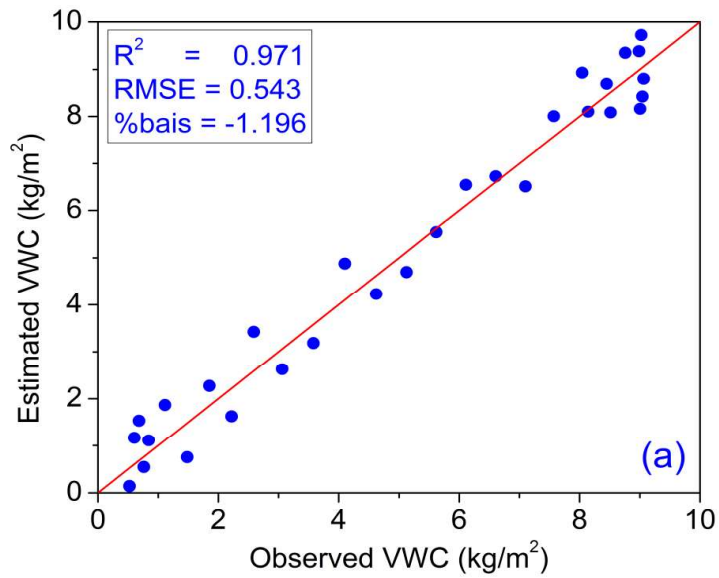


Figure 6.6 Flow chart for the estimation procedure of the wheat crop variables



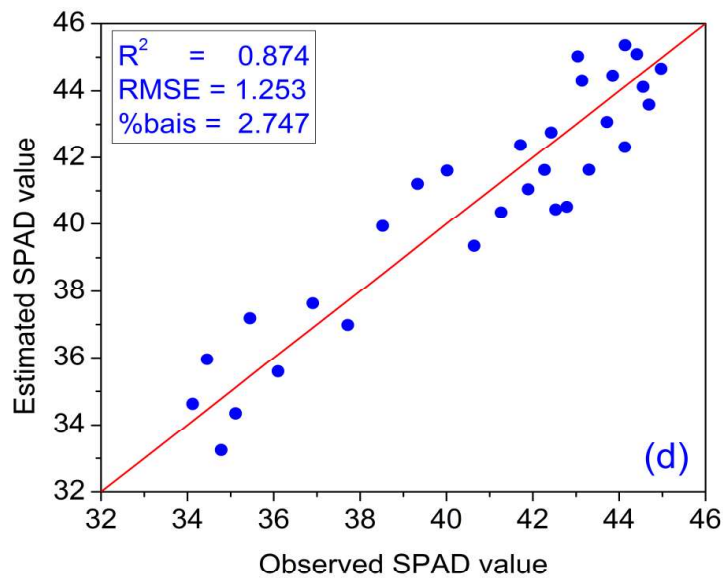
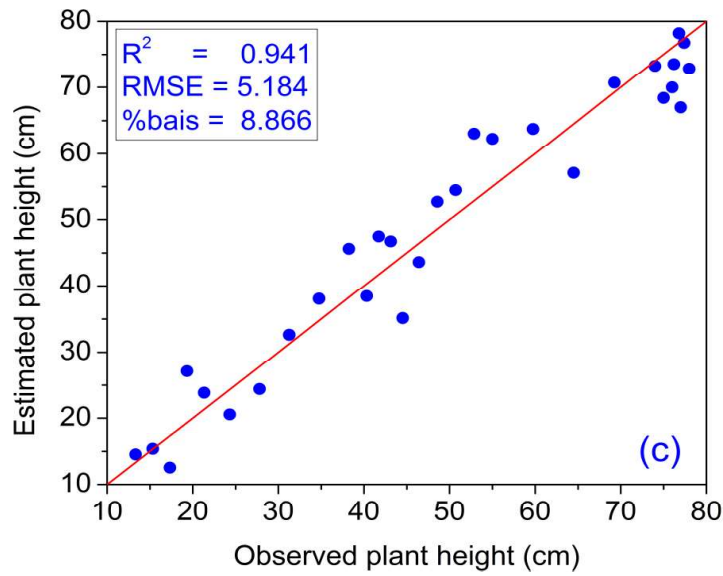
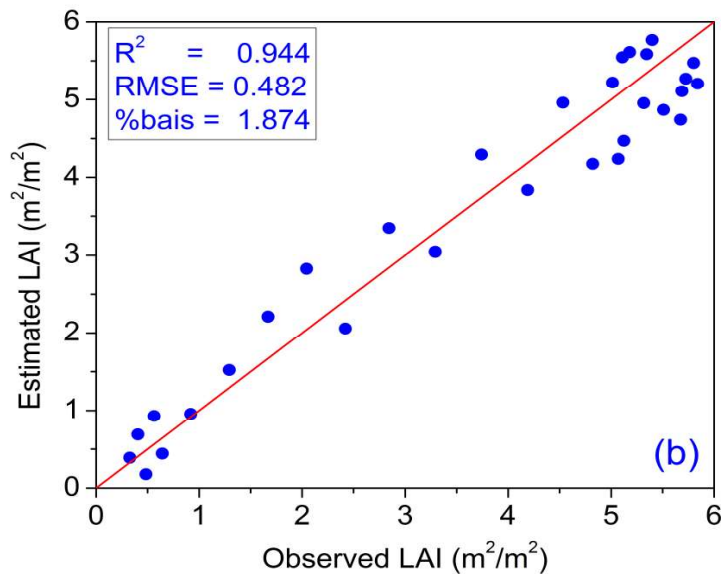
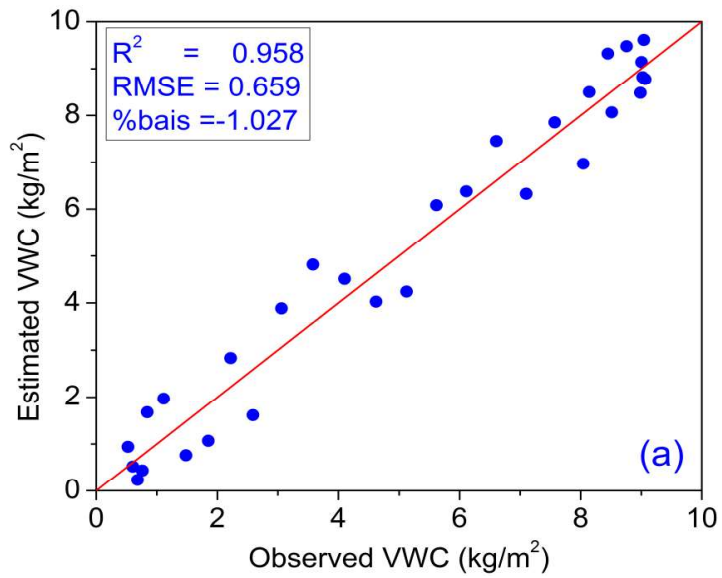


Figure 6.7 (a-d) 1:1 axes plot between estimated and observed crop variables for (a) VWC (b) LAI (c) PH and (d) SPAD value at HH- polarization.



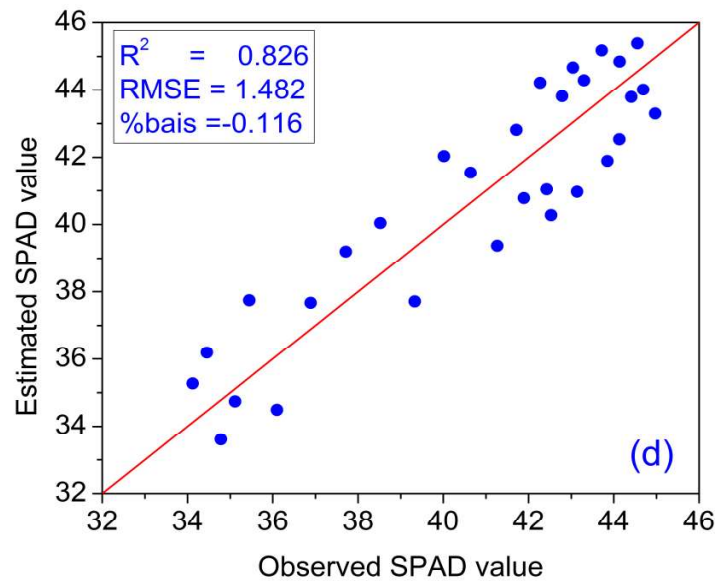
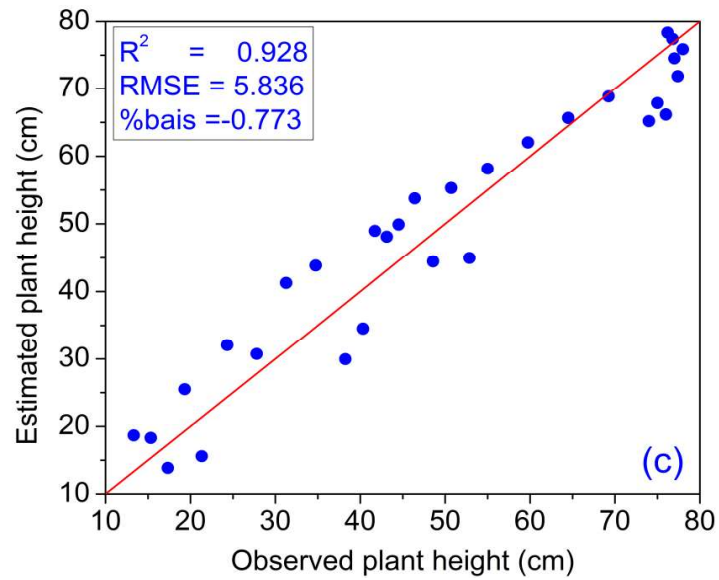


Figure 6.8 (a-d) 1:1 axes plot between estimated and observed crop variables for (a) VWC (b) LAI (c) PH and (d) SPAD value at VV- polarization.

6.5 CONCLUSIONS

The angular variation of bistatic scattering coefficients was found decreasing at all the growth stages of wheat crop. The 40° incidence angle at both HH- and VV-polarization was found suitable for the accurate estimation of wheat crop variables by the regression analysis. The estimated values by the ANN model for each crop variable were found very close to the observed values of crop variables. The estimation of VWC was found better in comparison to other crop variables at both polarizations. However, HH- polarization shows comparatively good results than the VV-polarization.